Spatiotemporal Variability Characteristics of Clear-Sky Land Surface Temperature in Urban Areas of Japan Observed by Himawari-8

Yuhei Yamamoto and Hirohiko Ishikawa

Disaster Prevention Research Institute, Kyoto University, Kyoto, Japan

Abstract

This paper provides the first attempt to investigate the spatial variability of diurnal change patterns of land surface temperature (LST) in urban areas of Japan by applying principal component analysis on LST data retrieved from Himawari-8 geostationary satellite data. The Tokyo and Osaka metropolitan areas were the focus of the analysis, and the target days were days with zero cloud cover in summer and winter. The results of the analysis showed that diurnal cycles of LST are mainly formed by two temporal change patterns in both seasons. For the summer case, the first two principal components (PCs) represented the temporal change patterns related to the amplitude and phase, respectively. For the winter case, the first two PCs represented the temporal change patterns related to the amplitude and gradual change in LST throughout the day, respectively. Results suggest that these temporal change patterns in both seasons have spatial variability partially dictated by land use and wind speed/direction.

(**Citation**: Yamamoto, Y., and H. Ishikawa, 2018: Spatiotemporal variability characteristics of clear-sky land surface temperature in urban areas of Japan observed by Himawari-8. *SOLA*, **14**, 179−184, doi:10.2151/sola.2018-032.)

1. Introduction

Land surface temperature (LST) is one of the key parameters in land-atmosphere interactions at various scales. LST observations have been used to monitor land cover change processes due to deforestation and urbanization (Sobrino and Raissouni 2000; Honjo et al. 2017), and to study environmental issues such as desertification or the urban heat island (Hung et al. 2006; Weng 2009; Li et al. 2013a). Specifically, in LST observation for urban areas, ground observation by radiation thermometer (Sugawara and Kondo 1995) and observation by polar-orbiting satellites and aircrafts (Weng 2009; Li et al. 2011; Connors et al. 2013; Xu et al. 2013; Honjo et al. 2017) are commonly performed due to their high spatial resolution (generally less than 1.1 km). Ground-based radiation thermometers can be used to observe the diurnal change of LST although the observation range is limited to a small part of an urban area. In contrast, polar-orbiting satellites and aircrafts can observe the LST in wider range but at lower temporal resolutions (over 12 hours).

Conditions in an urban hot environment are commonly evaluated using surface air temperature (SAT) or LST data (Memon et al. 2009). As the SAT ground observation network is substantial, SAT spatial and temporal change characteristics have been investigated in various cities with results showing that there are various diurnal change patterns in an urban area (e.g. Kim and Baik 2005; Suzuki and Iizuka 2009; Oku and Masumoto 2014; Santamouris 2015). Although the involved processes of LST and SAT are different, they are closely related. Therefore, it can be expected that the diurnal change pattern of the LST varies depending on not only surface materials but also the urban configurations and geographical characteristics.

Himawari-8 is a Japanese new-generation geostationary satellite that began recording observations in July 2015 (Bessho et al. 2016). Himawari-8 features very high temporal resolution (10 min) and relatively high spatial resolution (about 2 km) which is approximately equivalent to the ground observation network of SAT in Japanese metropolitan areas. Hence, the high spatial resolution of Himawari-8 renders it an ideal tool to observe the spatiotemporal characteristics of LST in urban areas.

In this letter, we retrieved the diurnal change of LST in urban areas from Himawari-8 data and investigated the different types of spatiotemporal variability characteristics seen in the retrieved LST. This study marks the first attempt to use geostationary satellite data for the study of urban LST diurnal change characteristics. As such, the main aims are to prove the applicability of Himawari-8 data in urban observation and to show how it can be used to provide new insights on related issues such as the impact of urban configurations and geographical characteristics on LST.

2. Data and method

2.1 LST data

LST was retrieved from Himawari-8 thermal infrared (TIR) band data. The spatial resolution of the TIR bands, and therefore the resolution of LST data are 0.02°. The observation cycle is 10 min for the full disk. For the Multifunction Transport Satellite (MTSAT) data, a non-linear split-window algorithm (NSW), which uses the difference between brightness temperatures measured in two TIR bands, was used to retrieve LST (Takeuchi et al. 2012). Yamamoto et al. (2018) developed a non-linear three-band algorithm (NTB) that makes the best use of three TIR bands of Himawari-8 (centered at 10.4, 11.2 and 12.4 μm). They showed that the NTB has higher accuracy than the NSW when dealing with hot and humid environments, such as is typical of many areas in Japan. Hence, we retrieved LST by using the NTB. The NTB requires the brightness temperatures and land surface emissivities (LSEs) of three TIR bands. LSEs were estimated using the method developed by Yamamoto and Ishikawa (2018), which is a combination of the classification-based method and the normalized difference vegetation index thresholds method (Li et al. 2013b). LST was estimated hourly in order that the characteristics of the diurnal change of LST can be fully grasped. As TIR radiation cannot be transmitted through clouds, this algorithm can only be applied to clear-sky pixels. The clear-sky pixels were extracted using the cloud detection method developed by Yamamoto et al. (2018). The LST estimation accuracy relies on the reliability of cloud detection, LSE estimation, Himawari-8's sensor and atmospheric correction.

2.2 Areas

The area that was analyzed covered the Tokyo metropolitan area, which includes the central urban area of Tokyo and surrounding suburbs of nearby prefectures (see Fig. 1a). The area is located in the Kanto plain and is the most urbanized location in Japan. The analyzed area did not include highly vegetated areas such as forests, but it did include urban green areas and agricultural areas.

Days with zero cloud cover in summer and winter were the primary target days. We avoided using multi-day composite LST data that included temporarily sunny days. This is because the noise stemming from the misjudgment of the cloud detection and the influence of clouds on the radiation balance of the land

---

Corresponding author: Yuhei Yamamoto, Kyoto University, Uji, Kyoto 611-0011 Japan. E-mail: yamamoto_y@storm.dpri.kyoto-u.ac.jp
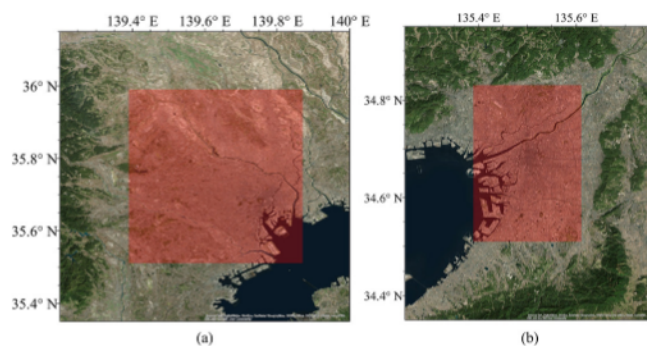
Fig. 1. The analyzed areas of (a) Tokyo metropolitan area which includes the central urban area of Tokyo and its surrounding suburbs of nearby prefectures (139.39°E−139.87°E, 35.51°N−35.99°N) and (b) Osaka metropolitan area (135.39°E−135.61°E, 34.51°N−34.83°N). Images shown from Google Earth.

surface, which are different from day to day, make it difficult to extract continuous time-change components of a sunny day. The target days in summer and winter were selected between the period of July 2015 and January 2018. The final selected dates were 5 August 2015 and 11 February 2016.

The number of applicable pixels in the 576-pixel target area were 369 and 532 pixels, respectively, as shown in Fig. 1a (see Figs. 3a and 3c). Applicable pixels are pixels that are judged to be cloud-free for 24 hours by cloud detection and have a small percentage of water surface (less than 50%). During winter in the Kanto plain, there was one day when almost all the pixels of the target area were applicable. In contrast, during the summer, clouds associated with the sea-breeze front are easily generated because the circulation of land and sea breezes becomes active on sunny days. Therefore, there is no day when all the pixels in the target area were cloud-free all day, and we selected the day on which had the most applicable pixels. The retrieved LSTs in summer case may include the noise of cloud contamination due to misjudgment of the cloud detection. Hence, in order to obtain better consideration avoiding misunderstanding due to the noise, we also investigated LSTs over the Osaka metropolitan area for the summer as a comparison target.

The Osaka metropolitan area is another highly urbanized city in Japan and is located in the Osaka plain (Fig. 1b). Because the Osaka plain is smaller than the Kanto plain, the influence of clouds generated from the sea-breeze front is smaller. The day chosen for the analysis was 12 August 2016. The number of applicable pixels was 157 of 176 pixels of the target area as shown in Fig. 1b (see Fig. 3b).

2.3 Analysis method

Principal component analysis (PCA) is a multivariate analysis method that compresses multidimensional data into fewer dimensions (North et al. 1982). PCA has been widely applied in previous studies as a method for extracting principal temporal change patterns from the time series data of SAT observed at multiple points (Kim and Baik 2005; Suzuki and Iizuka 2009; Oku and Masumoto 2014).

Here, we applied PCA in a similar way, but using LST, to extract principal temporal change patterns and study its spatial variability characteristics in an urban area. LST values were converted to their deviations from the daily mean LST of each pixel. These data were regarded as multivariate data with 24-dimensional variables for each pixel and were used as input data for PCA. By solving the eigenvalue problem of the variance–covariance matrix of the input data, the eigenvalues (Table 1) and eigenvectors (Fig. 2) of each principal component (PC) were calculated. The eigenvector denotes the temporal function. The PC score, which is determined for each pixel (Fig. 3), was calculated as the scalar product of the input data and the eigenvector.

After running the PCA for the three cases (Tokyo in summer and winter, and Osaka in summer), the errors of the eigenvalues caused by the number of pixel fluctuations were checked using the rule of thumb proposed by North et al. (1982). It was judged that the first, second and third PCs (PC1, PC2 and PC3) are independent of each other. In this study, we considered PC1 and PC2 that have eigenvalues of more than 1.0.

3. Results

Overall, the magnitudes of the eigenvalues and eigenvectors of PC1 and PC2 for Tokyo and Osaka in the summer were almost identical (see Table 1 and Fig. 2). Small differences, such as the sudden changes in the PC2 eigenvectors between 0:00 and 2:00

Table 1. Eigenvalues and contribution ratios derived in PCA.

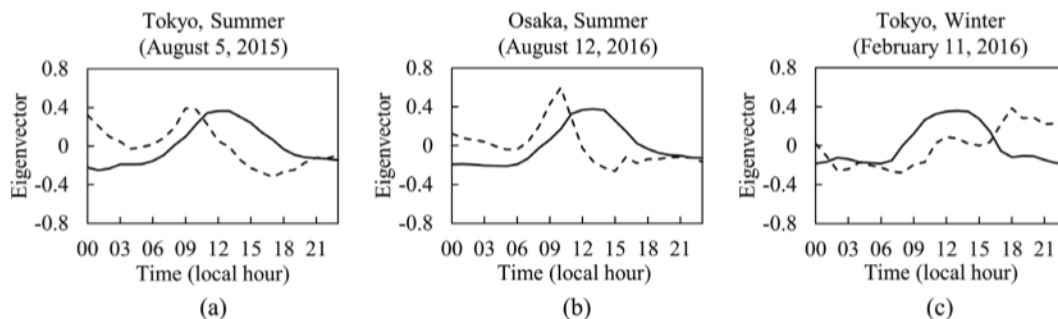| Principal Component	Tokyo, Summer (August 5, 2015)		Osaka, Summer (August 12, 2016)		Tokyo, Winter (February 11, 2016)	
	Eigenvalue	Contribution Ratio	Eigenvalue	Contribution Ratio	Eigenvalue	Contribution Ratio
PC1	18.96	76.61%	18.28	80.04%	12.98	71.65%
PC2	1.71	6.92%	1.70	7.45%	1.58	8.74%
PC3	0.97	3.94%	0.93	4.09%	0.76	4.23%
PC4	0.64	2.58%	0.49	2.15%	0.56	3.11%
PC5	0.48	1.95%	0.32	1.39%	0.44	2.42%

Fig. 2. The eigenvectors of PC1 and PC2 of (a) summer in Tokyo, (b) summer in Osaka and (c) winter in Tokyo. Solid lines display the eigenvectors of PC1 and dashed lines display the eigenvectors of PC2.

for Tokyo and between 15:00 and 17:00 for Osaka, however, were noted. These sudden changes might have been caused by cloud contamination due to misjudgment of cloud detection since the temporal LST changes during these times would not suddenly change.

The eigenvectors of PC1 in summer and winter represent the same temporal change that takes positive maxima around the noon and becomes negative during the nighttime. The eigenvectors of PC2 in summer take positive maxima from 9:00 to 10:00 and negative maxima from 15:00 to 17:00, whereas in winter it monotonically increases throughout the day.

Figure 3 shows the spatial distribution of PC scores of each PC and the land use distribution for each analyzed area. The PC score represents the degree of temporal change represented by each PC. To show the temporal change characteristics represented by each PC in more detail, we compared the diurnal LST changes for pixels that had the five highest PC scores and the five lowest PC scores in each analyzed area (Fig. 4). For PC1 in summer and winter, pixels with high scores had large diurnal ranges (approximately 30°C), whereas pixels with low scores had small diurnal ranges (approximately 15°C). For PC2 in summer, a difference in diurnal ranges could not be detected, despite the difference in

timing of maximum LSTs. For PC2 in winter, the LST difference gradually increased throughout the day.

4. Discussion

4.1 Diurnal change patterns of LST in summer

Judging from the eigenvectors (Figs. 2a and 2b), PC1 corresponds to the amplitude of the diurnal cycle. The LST differences between high and low PC scores became noticeable in the daytime reaching about 10°C in both areas (Figs. 4a and 4b). The pixels occupied by low buildings in inland had high PC scores, and the pixels occupied by high buildings or vegetation had low PC scores (Figs. 3a, 3b and Table 2).

The amplitude of the diurnal cycle would be related to the thermal inertia. The thermal inertia is a thermal and physical property indicating the degree of resistance to a temperature change of a surface material. The larger thermal inertia leads to the smaller LST change, so that the amplitude of the diurnal cycle becomes smaller (Sugawara and Kondo 1995). High buildings mainly consist of concrete which have large thermal inertia, whereas the low buildings consist of wooden materials which have small thermal
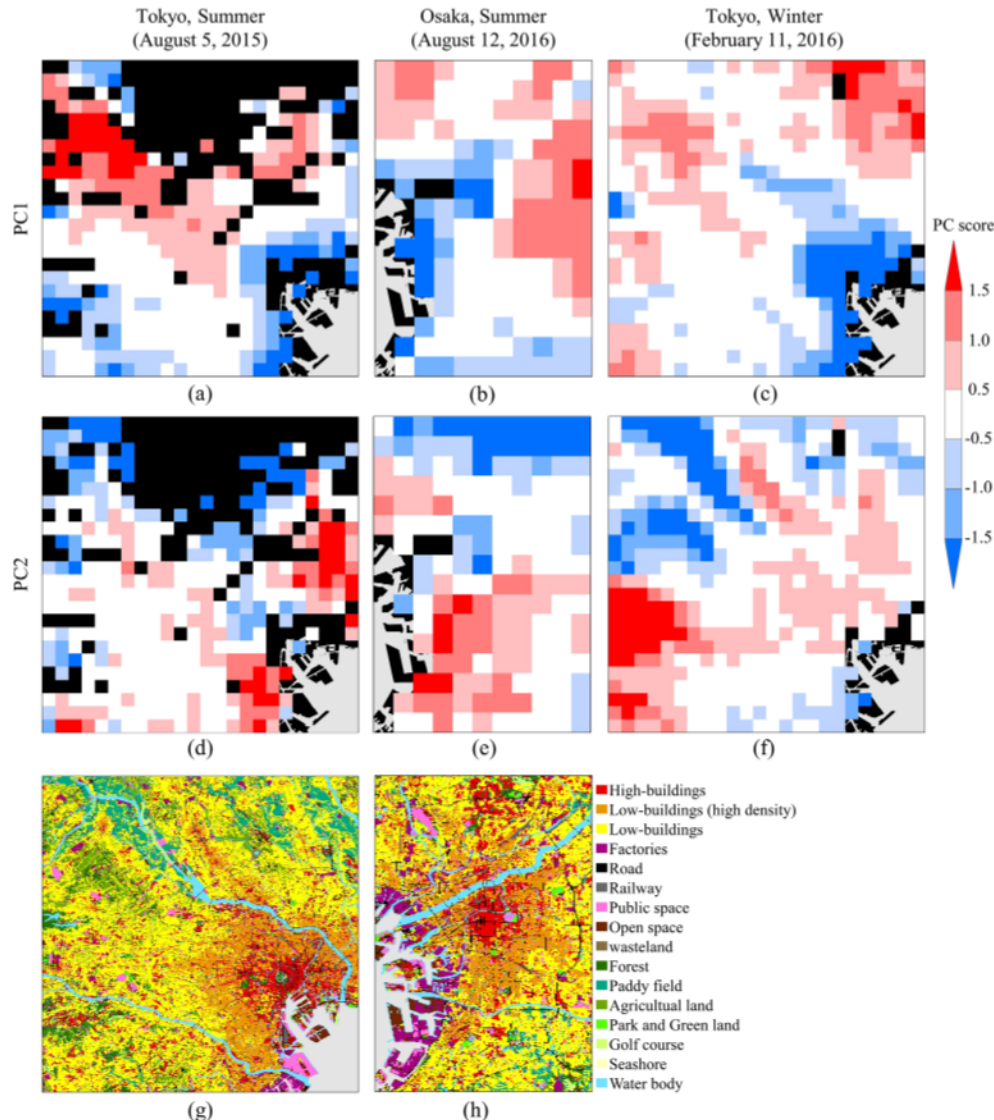

Fig. 3. First and second row depicts the spatial distributions of PC score of PC1 and PC2, respectively of (a, d) summer in Tokyo, (b, e) summer in Osaka and (c, f) winter in Tokyo. PC score is normalized. The third row depicts the urban area land use segmentation mesh data (100 m) of national land numerical information for (g) Tokyo and (h) Osaka areas provided by Ministry of Land, Infrastructure and Transport of Japan.
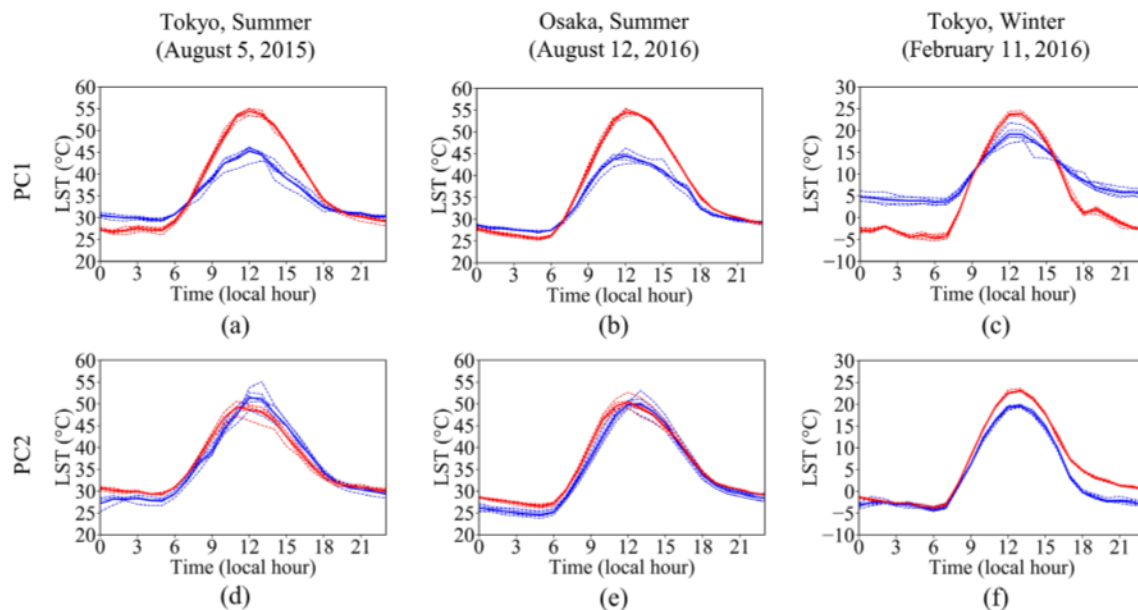
Fig. 4. The diurnal LST changes for pixels which are the five highest PC scores (red lines) and the five lowest PC scores (blue lines), of PC1 and PC2 of (a, d) summer in Tokyo, (b, e) summer in Osaka and (c, f) winter in Tokyo. Thin dashed lines are the LSTs of five high/low score pixels. Thick solid lines are the average values of LST at five high/low score pixels.

Table 2. Average PC scores and their deviations of pixels occupied (> 50%) by high buildings, low buildings (high density), low buildings (low density) and vegetation, respectively. Of all the pixels in each region, one third pixels closest to the coast were defined as "coastal" and one third pixels farthest from the coast were defined as "inland". The average scores greater than 0.5 are shaded in red and the scores less than −0.5 are shaded in blue.

			High buildings	Low buildings (high density)		Low buildings (low density)		Forest and agricultural land
				Coastal	Inland	Coastal	Inland	
Tokyo, Summer (August 5, 2015)	PC1	Ave.	−1.83	−0.28	0.82	0.01	0.89	−1.41
		Dev.	0.50	0.57	0.15	0.30	0.86	0.54
	PC2	Ave.	−0.60	1.13	0.25	0.49	−0.54	−1.58
		Dev.	0.49	0.76	0.38	0.21	0.87	1.09
Osaka, Summer (August 12, 2016)	PC1	Ave.	−1.61	0.33	1.43	−0.23	0.68	−0.63
		Dev.	0.09	0.15	0.04	0.67	0.66	0.34
	PC2	Ave.	−1.48	1.25	0.89	0.61	−0.36	−0.81
		Dev.	0.22	0.07	0.03	0.61	0.84	0.95
Tokyo, Winter (February 11, 2016)	PC1	Ave.	−2.65	−0.63	0.12	−0.44	0.64	0.13
		Dev.	0.34	0.62	0.45	0.27	0.48	0.93
	PC2	Ave.	0.38	0.13	0.57	−0.29	0.09	−1.33
		Dev.	0.28	0.39	0.27	0.33	1.06	1.22

inertia. (Li et al. 2011; Tsunematsu et al. 2016). As another factor, the building shadows may further lead to lower LST during daytime and smaller amplitude in regions occupied by high buildings. The water body also has high thermal inertia, so that pixels in coastal areas containing water surfaces had small amplitude. As the spatial characteristics, the PC score tended to be low in the coastal area and high in inland. The wind speed in the coastal area was higher than that in the inland during daytime (see Fig. S1). This strong wind in the coastal area enhance the convective heat transfer near the surface and may result in lower LST during daytime and smaller amplitude.

　　PC2 corresponds to the timing of the maximum LST in the diurnal cycle, i.e. phase shifting (Figs. 4d and 4e). The LST magnitude relationship between high and low PC scores is reversed between forenoon and afternoon. The pixels occupied by low buildings (high-density) had high PC scores, and pixels occupied by high buildings and paddy field had low PC scores (Figs. 3d, 3e

and Table 2). The phase shifting is considered to be related to the thermal inertia, similar to the PC1. It is interesting that the phase of a pixel occupied by high-density areas of low buildings tended to be fast, although it is understandable that the phases of pixels occupied by high buildings and paddy field including water body were slow since they have large thermal inertia. However, because there were some exceptions (e.g. a pixel occupied by high-density areas of low buildings where PC score is not high), the relationship between phase shifting and land use could not be noted as definitive.

　　As the spatial characteristics, the PC score tended to be high in the coastal areas and low in inland. This tendency may be related to the difference in the penetration time of sea breeze between coastal and inland areas. For example, as shown in Fig. S2, the penetration time of sea breeze, which was judged by the wind direction/speed changes and the SAT decrease, at Sakai located in the high PC score area was earlier than that of Osaka located

in low PC score area. However, the penetration times at Yao and Toyonaka located in the high PC score areas were almost same as that of Osaka. There was no clear relationship between PC2 and sea breeze in this analysis.

4.2 Diurnal change patterns of LST in winter

The winter PC1 represents information on the amplitude of the diurnal cycle, similar to the summer PC1 (Fig. 2). However, some differences in the spatial distribution of PC score were noted, especially in vegetation. The score of PC1 in vegetation for the winter was much higher than that for the summer (Table 2). This is because the amplitude of the diurnal cycle in vegetated areas changes as a function of decreasing transpiration and an increasing proportion of dry soil surface owing to fallen leaves in winter (Quan et al. 2014). The LST difference between high and low PC scores became larger in the nighttime reaching about 10°C. It is thought that the difference in heat storage effect due to thermal inertia was noticeable during nighttime. The wind speed during nighttime was stronger in the coastal area (Fig. S3), and it worked to reduce the LST difference between high and low PC scores (Fig. 3c).

The information represented by winter PC2 was different from that of summer PC2 (Fig. 2). It is thought that the phase difference becomes smaller as the length of daytime becomes shorter in winter. Also, in the vegetation area where the score of summer PC2 tends to be negative (i.e., slow phase), the thermal inertia becomes smaller and the phase becomes faster due to the decrease of soil moisture (Sugawara and Kondo 1995). The winter PC2 corresponds to a gradual change in LST throughout the day on a sunny day. Pixels occupied by paddy field and agricultural land had low PC scores (Fig. 3f and Table 2). This is because these land uses are in the fallow period and the heat storage effect become smaller than that of summer case due to the decrease of soil moisture. Furthermore, as shown in Fig. S3, the regions where the northwest wind was strong from night to dawn (e.g. Saitama and Tokorozawa) had small nocturnal cooling of SAT probably due to wind-induced mechanical destruction of stable stratification, which can have a lingering effect for LST change during the day. Overall, a region with low wind speed during midnight or daytime (e.g., Fuchu in Fig. S3) or high thermal inertia (e.g., high-buildings in Fig. 3g), which have high heat storage effect, might have high PC score.

5. Conclusions and perspectives

In this letter, we retrieved the diurnal changes of LST in Tokyo and Osaka metropolitan areas from Himawari-8 data and investigated the spatiotemporal variability characteristics seen in the retrieved LST by applying the PCA. The targeted days were days with zero cloud cover in summer and winter. The first two PCs in summer represented the temporal change patterns related to the amplitude and phase, respectively. In the winter, the first two PCs represented the temporal change patterns related to the amplitude and gradual change in LST throughout the day, respectively. These temporal change patterns for the days studied here in both seasons were confirmed to have spatial variability corresponding to land use and wind speed/direction.

The spatial distribution of the instantaneous LST observed by the polar-orbiting satellite/aircraft may vary depending on the spatial difference of the temporal changes of LST, such as the phase shifting (summer PC2) and LST change throughout the day (winter PC2). Therefore, urban observation considering the temporal changes of LST can provide more valuable discussions. As the amount of clear-sky days observed by Himawari-8 increase, we plan to use the method shown to study the detailed correlations between the temporal changes of LST, urban configurations and geographical characteristics.

Supplements

Figures S1, S2 and S3 show the time series of wind speed/direction and SAT observed at the stations of AMeDAS in the analysis areas and days.

References

Bessho, K., K. Date, M. Hayashi, A. Ikeda, T. Imai, H. Inoue, Y. Kumagai, T. Miyakawa, H. Murata, T. Ohno, A. Okuyama, R. Oyama, Y. Sasaki, Y. Shimazu, K. Shimoji, Y. Sumida, M. Suzuki, H. Taniguchi, H. Tsuchiyama, D. Uesawa, H. Yokota, and R. Yoshida, 2016: An introduction to Himawari 8/9 – Japan's new-generation geostationary meteorological satellites. *J. Meteor. Soc. Japan*, **94**, 151−183.

Connors, J. P., C. S. Galletti, and W. T. L. Chow, 2013: Landscape configuration and urban heat island effects: Assessing the relationship between landscape characteristics and land surface temperature in Phoenix, Arizona. *Landsc. Ecol.*, **28**, 271−283, doi:10.1007/s10980-012-9833-1.

Honjo, T., N. Tsunematsu, and H. Yokoyama, 2017: Urban climate analysis of urban surface temperature change using structure- from-motion thermal mosaicing. *Urban Climate*, **20**, 135−147, doi:10.1016/j.uclim.2017.04.004.

Hung, T., D. Uchihama, S. Ochi, and Y. Yasuoka, 2006: Assessment with satellite data of the urban heat island effects in Asian mega cities. *Int. J. Appl. Earth Obs. Geoinf.*, **8**, 34−48, doi:10.1016/j.jag.2005.05.003.

Kim, Y.-H., and J.-J. Baik, 2005: Spatial and temporal structure of the urban heat island in Seoul. *J. Appl. Meteor.*, **44**, 591−605, doi:10.1175/JAM2226.1.

Li, J., C. Song, L. Cao, F. Zhu, X. Meng, and J. Wu, 2011: Impacts of landscape structure on surface urban heat islands: A case study of Shanghai, China. *Remote Sens. Environ.*, **115**, 3249−3263, doi:10.1016/j.rse.2011.07.008.

Li, Z.-L., B. H. Tang, H. Wu, H. Ren, G. Yan, Z. Wan, I. F. Trigo, and J. A. Sobrino, 2013a: Satellite-derived land surface temperature: Current status and perspectives. *Remote Sens. Environ.*, **131**, 14−37, doi:10.1016/j.rse.2012.12.008.

Li, Z.-L., H. Wu, N. Wang, S. Qiu, J. A. Sobrino, Z. Wan, B.-H. Tang, and G. Yan, 2013b: Land surface emissivity retrieval from satellite data. *Int. J. Remote Sens.*, **34**, 3084−3127, doi:10.1080/01431161.2012.716540.

Memon, R. A., D. Y. C. Leung, and C. H. Liu, 2009: An investigation of urban heat island intensity (UHII) as an indicator of urban heating. *Atmos. Res.*, **94**, 491−500, doi:10.1016/j.atmosres.2009.07.006.

North, G. R., T. L. Bell, and R. F. Cahalan, 1982: Sampling errors in the estimation of empirical orthogonal funtions. *Mon. Wea. Rev.*, **110**, 699−706, doi:10.1175/1520-0493(1982)110 <0699:SEITEO>2.0.CO;2.

Oku, Y., and K. Masumoto, 2014: An observational study of the difference on urban heat islands between summer and winter in Osaka City. *J. Heat Isl. Inst. Int.*, **9**, 1−12 (in Japa-

nese).

Quan, J., Y. Chen, W. Zhan, J. Wang, J. Voogt, and J. Li, 2014: A hybrid method combining neighborhood information from satellite data with modeled diurnal temperature cycles over consecutive days. *Remote Sens. Environ.*, **155**, 257−274, doi:10.1016/j.rse.2014.08.034.

Santamouris, M., 2015: Analyzing the heat island magnitude and characteristics in one hundred Asian and Australian cities and regions. *Sci. Total Environ.*, **512−513**, 582−598, doi: 10.1016/j.scitotenv.2015.01.060.

Sobrino, J. A., and N. Raissouni, 2000: Toward remote sensing methods for land cover dynamic monitoring: Application to Morocco. *Int. J. Remote Sens.*, **21**, 353−366, doi:10.1080/014311600210876.

Sugawara, H., and J. Kondo, 1995: Sensitivity test of urban surface temperature. *Tenki*, **42**, 813−818 (in Japanese).

Suzuki, T., and Y. Iizuka, 2009: Diurnal temperature changing patterns of Tokyo according to season and weather. *Tenki*, **56**, 627−635 (in Japanese).

Takeuchi, W., K. Oyoshi, and S. Akatsuka, 2012: Super-resolution of MTSAT land surface temperature by blending MODIS and AVNIR2. *Asian J. Geoinformatics*, **12**, 47−51.

Tsunematsu, N., H. Yokoyama, T. Honjo, A. Ichihashi, H. Ando, and N. Shigyo, 2016: Relationship between land use vari-

ations and spatiotemporal changes in amounts of thermal infrared energy emitted from urban surfaces in downtown Tokyo on hot summer days. *Urban Climate*, **17**, 67–79, doi: 10.1016/j.uclim.2016.03.002.

Weng, Q., 2009: Thermal infrared remote sensing for urban climate and environmental studies: Methods, applications, and trends. *ISPRS J. Photogramm. Remote Sens.*, **64**, 335−344, doi:10.1016/j.isprsjprs.2009.03.007.

Xu, L. Y., X. D. Xie, and S. Li, 2013: Correlation analysis of the urban heat island effect and the spatial and temporal distribution of atmospheric particulates using TM images in Beijing. *Environ. Pollut.*, **178**, 102−114, doi:10.1016/j.envpol.2013.03.006.

Yamamoto, Y., and H. Ishikawa, 2018: Thermal land surface emissivity for retrieving land surface temperature from Himawari-8. *J. Meteor. Soc. Japan*, **96B**, 43−58, doi: 10.2151/jmsj.2018-004.

Yamamoto, Y., and H. Ishikawa, Y. Oku, and Z. Hu, 2018: An algorithm for land surface temperature retrieval using three thermal infrared bands of Himawari-8. *J. Meteor. Soc. Japan*, **96B**, 59−76, doi:10.2151/jmsj.2018-005.